CrystEngComm

Accepted Manuscript

ROYAL SOCIETY OF CHEMISTRY

www.rsc.org/crystengcomm

Journal Name

RSCPublishing

COMMUNICATION

C–H···H–C and C–H···π Contacts Aid Transformation of Dimeric to Monomeric Anthracene in the Solid State

Cite this: DOI: 10.1039/x0xx00000x

Kalaivanan Nagarajan, Shinaj K. Rajagopal and Mahesh Hariharan*

Received 00th January 2012,
Accepted 00th January 2012

DOI: 10.1039/x0xx00000x

www.rsc.org/

We report C–H···H–C and C–H···π interactions assisted formation of thermodynamically stable blue emissive AP-I from kinetically stable green emissive AP-II crystal polymorph of 1-(anthracen-9-yl)pyrene (AP). Rotational degree of freedom at the bond between two constituent chromophores facilitates the formation of conformational polymorphs AP-I and AP-II that can be quantitatively crystallized from ethylacetate and hexane respectively.

Organic solid-state luminescent materials received immense attention due to their promising optoelectronic applications as light-emitting diodes, lasers, sensors etc.[1] Tuning the luminescence properties of an organic material is an emerging area of interest.[2] Organic chromophores that exhibit strong fluorescence in solution could become non-fluorescent in the solid state due to exciton interactions. Chromophores such as anthracene may undergo photoaddition[3] due to the π–π stacked arrangement in the solid state.[4] Tilt–slide dimeric geometry of anthracene in the solid state can prevent photoaddition but limits the orbital overlap.[5] Photostable dimeric structure of anthracene in the solid state possessing extensive orbital overlap and favourable photophysical properties demands further attention.[6] Transition of dimeric to monomeric anthracene in the crystalline state can result in contrasting fluorescence properties.[7] Heat,[8] mechanical stress,[9] solvent vapour[10] induced interplay between weak interactions[11] such as π–π, C–H···π, and C–H···N/O/X could reversibly or irreversibly alter solid state packing and photophysical properties.[12] We report for the first time, C–H···H–C[13] and C–H···π contacts aided thermal transformation of kinetically stable dimeric to thermodynamically stable monomeric anthracene in the solid state.

Our continued efforts to understand the photophysical properties of near-orthogonal dyads in solution *vs.* solid/assembled[14] state prompted us to explore a novel dyad having anthracene and pyrene units. Suzuki coupling between pyrene-1-boronic acid and 9-bromoanthracene offered 1-(anthracen-9-yl)pyrene (AP) dyad in 80% yield (Scheme S1, Figures S1 and S2, Electronic Supplementary Information (ESI†)). Attempts to crystallize AP in dichloromethane (DCM) resulted in concomitant formation of i) needle-like ash white (AP-I) and ii) oblong pale-yellow (AP-II) crystals. Solvent optimization for the crystallization of AP resulted in competitive polymorphism offering AP-I from ethyl acetate and AP-II from hexane. The solubility of AP is found to be higher in ethylacetate (1.25 mg/mL) when compared to hexane (0.25 mg/mL).

AP-I crystallizes in solvent free orthorhombic space group Iba2, having torsional angle of 80° between the constituent anthracene (AN) and pyrene (PY) units (Figure 1A and Table S1, ESI†). Detailed analysis of the single crystal X-ray structure of AP-I (Figure S3A, ESI†) indicates an interplanar angle (Φ) of 45.7° and a distance (D) of 3.0 Å between the nearest pyrene units facilitated through C–H···π interactions (Figure S4A, ESI†). Nearest anthracene units also exhibit C–H···π interactions having Φ of 80.5° and D of 2.8 Å (S4B, ESI†).

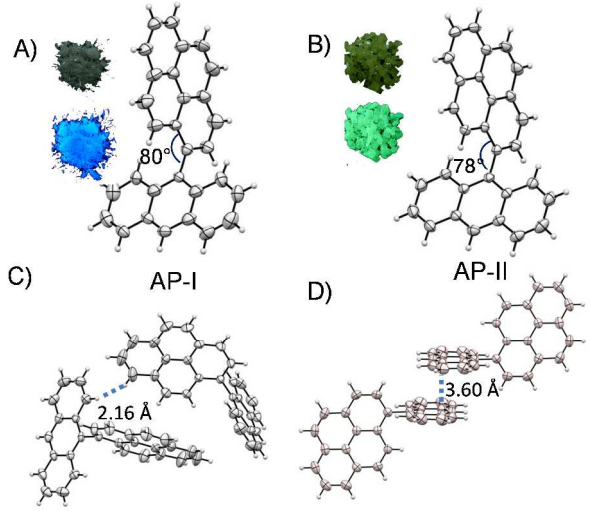

Figure 1. A) and B) single crystal X-ray structure of AP-I and AP-II respectively (percentage probability chosen for the ellipsoid is 20%): corresponding insets show the photographs under i) daylight (top) ii) UV illumination (bottom); C) intermolecular H···H interaction in AP-I and D) π–π interaction in AP-II.

We observed dihydrogen (C–H···H–C) interaction between nearest AN and PY moieties at a *D* of 2.16 Å (double of van der Waal's radius of hydrogen atom is 2.4 Å)[15] and *Φ* of 54.9° (Figure 1C). C–H···H–C contact also exists between two AN units at *Φ* of 73.7° and *D* of 2.3 Å (Figure S4C, ESI†). Quantum theory of atoms in molecules (QTAIM) analysis of AP-I confirmed the existence of C–H···H–C and C–H···π contacts (Figure S5, ESI†). A closed-shell intermolecular[16] homopolar C–H···H–C interaction between two nearest AN units evaluated substantial accumulation of electron density, $\rho_b(r)$ (0.0055 eÅ^{-3}) and the positive value of the Laplacian at the BCP (0.023 eÅ^{-5}; Table S2, ESI†). QTAIM analysis also confirmed C–H···H–C and C–H···π interactions between nearest AN and PY units in AP-I.

AP-II crystallizes in solvent free monoclinic space group P2(1)/c, with a torsional angle of 78° between AN and PY units (Figure 1B, Table S1, ESI†). Apart from C–H···π interactions (Figures S3B and S6A, ESI†) between AN and PY (*D*=2.80 Å; *Φ*=66°), we observed π–π (face-face) interactions between AN units at *D* of 3.6 Å, *Φ* of 2.20° and a transverse shift of 0.93 Å (Figure 1D). Facilitated through π–π interactions, nearest PY units were found at *D* of 3.30 Å, *Φ* of 0.36° and a transverse shift of 6.5 Å (Figure S6B, ESI†). Orbital overlap through π–π contacts between the AN/PY units can result in ground and/or excited state interactions in AP-II. We employed Hirshfeld analyses[17] to determine the ratio (ρ)[18] of %C···H and %C···C interactions in AP-I and AP-II (Figure S7 and Table S3, ESI†). Albeit herringbone structure (ρ>4.5) in AP-I and AP-II, a significant decrease in the ρ-value of AP-II (10.02) when compared to AP-I (27.39) indicates the presence of AN dimers in AP-II that is non-existent in AP-I.

Differential scanning calorimetric (DSC) analysis in AP-I shows an endothermic peak (ΔH = 32.2 J/mol) at 250°C corresponding to the melting transition of AP-I. AP-II exhibits a weakly endothermic peak (ΔH = 2.2 J/mol) at 233°C that corresponds to the enantiotropic transition[19] (see ESI†) of AP-II→AP-I followed by a strong endothermic peak (ΔH = 26.2 J/mol) at 250°C that corroborates to the melting transition of AP-I (Figure S8, ESI†). AP-II appears to be kinetically stable while AP-I is thermodynamically favored through additional C–H···H–C and C–H···π contacts. Upon melting AP-I and AP-II, the resultant solids exhibit powder X-ray diffraction (PXRD) pattern similar to AP-I (Figure 2), consistent with DSC.

UV-Vis absorption of AP in chloroform exhibits four narrow bands centered at 320, 340, 370 and 390 nm that are red-shifted when compared to the cumulative absorption bands of AN and PY in chloroform (Figure 3A and S9, ESI†). Upon excitation at 350 nm, AP shows a broad emission spectrum (400-550 nm), with quantum yield (Φ_{fl}) of 0.8. Red-shift corresponding to the emission of AP when compared to the constituents AN and PY in chloroform, consistent with UV-Vis data, confirms the extended conjugation in the dyad AP (Figure 3B and S10, ESI†). Excitation spectrum collected at 420 nm shows the involvement of AN and PY units in the fluorescence of AP (Figure 3C).[20] Upon excitation at 377 nm, picosecond time-resolved fluorescence measurement of AP in chloroform exhibits monoexponential decay when monitored at 420 nm with a lifetime of 4.7 ns (Figure 3D and Table S4, ESI†).

Crystalline AP-I and AP-II show distinct photophysical properties due to diverse packing that arises from conformational polymorphism. AP-I shows a broad UV-Vis absorption ranging between 300-440 nm whereas AP-II extends upto 480 nm (Figure 3A). A significant red-shift in the UV-Vis spectrum of AP-II when compared to the solution suggests the possibility of stronger ground state interactions. Upon excitation at 350 nm, AP-I exhibits three emission maxima centered at 410, 420 and 460 nm having Φ_{fl} of 0.3 (Figure 3B). Emission maximum of AP-I is marginally red-shifted as

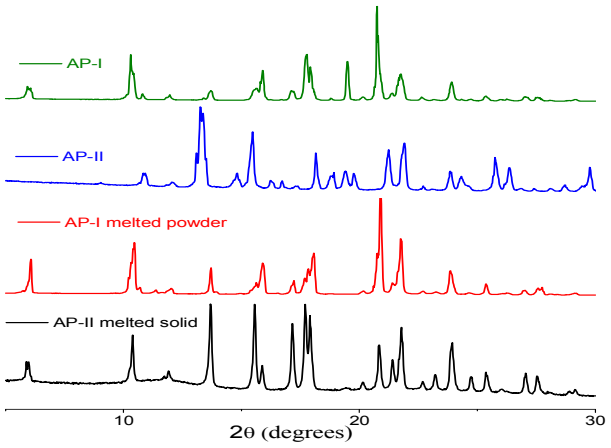

Figure 2. PXRD pattern of AP-I and AP-II before and after melting.

compared to monomeric AP in chloroform indicating the possibility of weak interaction in the solid state, consistent with UV-Vis data. Monomer-like emission and excitation spectra (Figure 3C and Figure S11A, ESI†) corroborate with the blue solid state emission of AP-I. A combination of i) C–H···π; ii) C–H···H–C contacts and iii) near-orthogonality (intra/intermolecular) between the constituents resulted in the monomeric nature of AN and PY units in AP-I.

Upon excitation at 350 nm, apart from weak monomer-like emission at 420 nm AP-II exhibits a broad emission at 520 nm having an overall Φ_{fl} of 0.4 (Figure 3B). Excitation wavelength independent emission at 520 nm (Figure S11B, ESI†) could be attributed to emission from aggregated,[5] either in the ground or excited, AN/PY units in AP-II. Excitation spectra of AP-II monitored at 420 nm (Figure 3C) was found to be identical with monomeric AP in solution. While monitored at 520 nm, excitation spectrum of AP-II exhibits strongly red-shifted broad band (ca. 50 nm) at 440 nm when compared to the excitation spectrum of monomeric AP in solution (Figure 3C). Large Stokes shift having a broad band in the crystalline AP-II excludes the possibility of 'J'

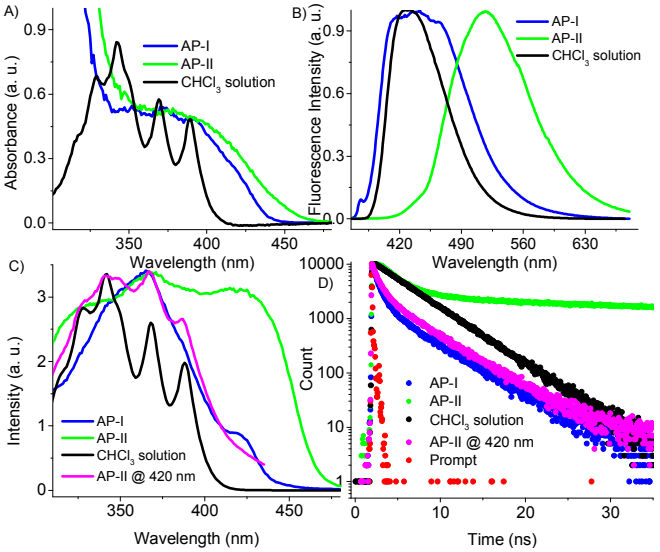

Figure 3. A) UV-Vis absorption; B) emission, excited at 350 nm; C) excitation spectra of the AP-I/II, AP in $CHCl_3$ (solution) monitored at 420 nm and AP-II monitored at 520 nm and D) fluorescence decay for AP-I/II, AP in $CHCl_3$ (solution) monitored at 420 nm and AP-II monitored at 560 nm (Figure S13, ESI† for complete decay).

aggregate. Faster rate of radiative decay of AP in solution as compared to crystalline AP-II indicates the formation of H-like aggregates and/or excimer in crystals. Existence of electron density in both the chromophoric units of HOMO/LUMO in AP-II, obtained using frontier molecular orbital (FMO) analysis, suggests the possibility of extended conjugation between AN and PY units in AP-II. While the HOMO/LUMO of AP-I indicates localized electron density in either AN/PY (Figure S12, ESI†).

Upon excitation at 377 nm, AP-I shows biexponential decay with lifetimes of 6.4 ns (75%) and 1.6 ns (25%) when monitored at 470 nm; 4.3 ns (30%) and 0.8 ns (70%) when monitored at 420 nm (Figure 3D and Table S4, ESI†). Similar lifetime for AP-I (4.3 ns) and AP (4.7 ns) in chloroform when monitored at 420 nm confirms the monomer-like behavior of constituents in AP-I. Moderate increase in the lifetime monitored at 470 nm in AP-I could arise from environmental heterogeneity. When monitored at 560 nm, AP-II shows a biexponential decay with the lifetimes of 96 ns (92%) and 4.2 ns (8%) (Figure S13, ESI†). Upon monitoring at 420 nm, we observed a biexponential decay (Figure 3D) with lifetimes of 5.0 ns (18%) and 1.8 ns (82%) corresponding to monomeric emission of AP-II in agreement with the steady state fluorescence. Longer lifetime of 80-96 ns in AP-II upon monitoring at 475-560 nm band is clearly indicative of the existence of AN and/or PY based aggregate, consistent with crystal structure (Figure S11B, ESI†). Reversible solvent vapour dependent emission was observed in AP-I and AP-II. Blue emissive AP-I turns to greenish blue emissive on exposure to hexane vapour (Figure S14A, ESI†) while green emissive AP-II turns to blue emissive on exposure to ethylacetate vapour (Figure S14B, ESI†). PXRD pattern before and after solvent exposure suggests non-significant change in the global molecular arrangement (Figure S15, ESI†). Localized reorganization of the molecular packing exclusively on the surface without altering the overall crystal structure upon exposure to vapours could result in the observed fluorescence shift. Gradual evaporation of the vapour resulted in blue and green emission of AP-I and AP-II respectively indicating the reversible fluorescence properties of polymorphs when exposed to solvent vapours. Exposure of AP-I and AP-II to ethylacetate and hexane respectively indicated negligible change in the emission (Figure S14C and D, ESI†).

In conclusion, we demonstrate the isolation of polymorphs AP-I and AP-II from ethyl acetate and hexane respectively. The conformational polymorphs AP-I and AP-II exhibit diverse photophysical properties due to their molecular packing in the crystal. C–H···H–C and C–H···π contacts, as confirmed through QTAIM analysis, makes the dyad to be monomer emissive (τ_f ~ 4.3 ns) in AP-I whereas π–π interaction develops dimer-/excimer-like (τ_f ~ 96 ns) emission in the AP-II. Kinetically stable AP-II can transform to thermodynamically stable AP-I upon heating. Solvent vapour induced fluorescence response of AP-I and AP-II makes the polymorphs interesting material for optoelectronic and sensor applications.

Acknowledgement

M. H. acknowledges the Science and Engineering Research Board for the support of this work, SERB/F/0962. Authors thank Mr. Alex P. Andrews for X-ray crystal structure analysis and Mr. Syed M. Bilal for partial assistance in the synthesis.

Notes and references

*School of Chemistry, Indian Institute of Science Education and Research Thiruvananthapuram, CET Campus, Sreekaryam, Thiruvananthapuram, Kerala, INDIA 695016. E-mail: mahesh@iisertvm.ac.in

† Electronic Supplementary Information (ESI) available: Tables of crystal data, Synthesis, characterization, photophysical and computational studies of AP-I and AP-II. CCDC reference numbers: 1001196-1001197. For ESI and crystallographic data in CIF, See DOI: 10.1039/c000000x/

1. D. Yan and D. G. Evans, *Mater. Horiz.*, 2014, **1**, 46-57.
2. (a) S. Varughese, *J. Mater. Chem. C*, 2014, **2**, 3499-3516; (b) S. Varghese and S. Das, *J. Phys. Chem. Lett.*, 2011, **2**, 863-873.
3. (a) H. Bouas-Laurent, A. Castellan, J.-P. Desvergne and R. Lapouyade, *Chem. Soc. Rev.*, 2000, **29**, 43-55; (b) B. Bibal, C. Mongin and D. M. Bassani, *Chem. Soc. Rev.*, 2014, 10.1039/C1033CS60366K.
4. T. Hinoue, Y. Shigenoi, M. Sugino, Y. Mizobe, I. Hisaki, M. Miyata and N. Tohnai, *Chem.-Eur. J.*, 2012, **18**, 4634-4643.
5. B. Dong, M. Wang, C. Xu, Q. Feng and Y. Wang, *Cryst. Growth Des.*, 2012, **12**, 5986-5993.
6. M. Sugino, Y. Araki, K. Hatanaka, I. Hisaki, M. Miyata and N. Tohnai, *Cryst. Growth Des.*, 2013, **13**, 4986-4992.
7. J. Bernstein, R. J. Davey and J.-O. Henck, *Angew. Chem. Int. Ed.*, 1999, **38**, 3440-3461.
8. R. Davis, N. P. Rath and S. Das, *Chem. Commun.*, 2004, 74-75.
9. C. Y. K. Chan, J. W. Y. Lam, Z. Zhao, S. Chen, P. Lu, H. H. Y. Sung, H. S. Kwok, Y. Ma, I. D. Williams and B. Z. Tang, *J. Mater. Chem. C*, 2014, **2**, 4320-4327.
10. A. V. Trask, N. Shan, W. D. S. Motherwell, W. Jones, S. Feng, R. B. H. Tan and K. J. Carpenter, *Chem. Commun.*, 2005, 880-882.
11. S. Long, S. Parkin, M. Siegler, C. P. Brock, A. Cammers and T. Li, *Cryst. Growth Des.*, 2008, **8**, 3137-3140.
12. (a) S. Tothadi and G. R. Desiraju, *Chem. Commun.*, 2013, **49**, 7791-7793; (b) T. Mutai, H. Satou and K. Araki, *Nat. Mater.*, 2005, **4**, 685-687; (c) A. Nangia, *Acc. Chem. Res.*, 2008, **41**, 595-604; (d) M. Brinkmann, G. Gadret, M. Muccini, C. Taliani, N. Masciocchi and A. Sironi, *J. Am. Chem. Soc.*, 2000, **122**, 5147-5157; (e) F. D. Lewis and J.-S. Yang, *J. Phys. Chem. B*, 1997, **101**, 1775-1781.
13. S. K. Rajagopal, A. M. Philip, K. Nagarajan and M. Hariharan, *Chem. Commun.*, 2014, **50**, 8644 - 8647.
14. (a) R. T. Cheriya, A. R. Mallia and M. Hariharan, *Energy Environ. Sci.*, 2014, **7**, 1661-1669; (b) R. T. Cheriya, K. Nagarajan and M. Hariharan, *J. Phys. Chem. C*, 2013, **117**, 3240-3248.
15. V. I. Bakhmutov, *Dihydrogen Bond: Principles, Experiments, and Applications*, John Wiley & Sons, Inc., Hoboken, New Jersey, 2008.
16. A. Volkov, P. Macchi, L. J. Farrugia, C. Gatti, P. R. Mallinson, T. Richter and T. Koritsanszky, User Manual, 2006 edn., vol. XD2006, a computer program package for multipole refinement, topological analysis of charge densities and evaluation of intermolecular energies from experimental or theoretical structure factors, pp. User Manual, 2006.
17. S. K. Wolff, D. J. Grinwood, J. J. McKinnon, M. J. Turner, D. Jayatilaka and M. A. Spackman, University of Western Australia, Perth, Australia, 2012.
18. L. Loots and L. J. Barbour, *CrystEngComm*, 2012, **14**, 300-304.
19. K. Kawakami, *J. Pharm. Sci.*, 2007, **96**, 982-989.
20. B. Kim, Y. Park, J. Lee, D. Yokoyama, J.-H. Lee, J. Kido and J. Park, *J. Mater. Chem. C*, 2013, **1**, 432-440.

Journal Name RSCPublishing

COMMUNICATION

Table of Contents: Graphical Abstract

C–H···H–C and C–H···π Contacts Aid Transformation of Dimeric to Monomeric Anthracene in the Solid State

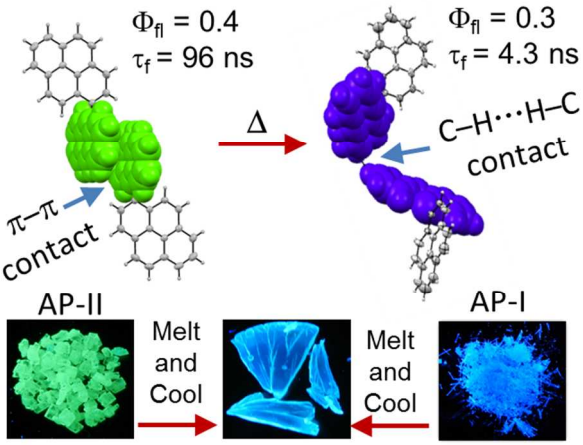

C–H···H–C and C–H···π interactions assisted formation of thermodynamically stable blue emissive AP-I from kinetically stable green emissive AP-II of 1-(anthracen-9-yl)pyrene (AP).